Journal of Alloys and Compounds 508 (2010) 115–118

Contents lists available at ScienceDirect

Journal of Alloys and Compounds

journal homepage: www.elsevier.com/locate/jallcom

Effect of La^{3+} doping on the electric, dielectric and magnetic properties of cobalt ferrite processed by co-precipitation technique

Pawan Kumar [a,*], S.K. Sharma [b], M. Knobel [b], M. Singh [a]

[a] Department of Physics, Himachal Pradesh University, Shimla, India
[b] Low Temperature Laboratory, Instituto de Física Gleb Wataghin (Physics Institute), Campinas, Sao Paulo, Brazil

ARTICLE INFO

Article history:
Received 12 May 2010
Received in revised form 4 August 2010
Accepted 4 August 2010
Available online 11 August 2010

PACS:
77.22.Gm
75.60.Ej
77.22.Gm
72.15.Eb

Keywords:
Nano-structures
Chemical synthesis
X-ray diffraction
Dielectric response
Magnetic measurements

ABSTRACT

Lanthanum doped cobalt ferrite ferrites with improved dielectric and magnetic properties have been synthesized by co-precipitation technique. The nano-structures, dielectric and magnetic properties have been investigated by means of X-ray diffraction, impedance analyzer and VSM respectively. The dielectric properties and magnetic properties of $CoLa_xFe_{2-x}O_4$ ($x = 0$, 0.1, 0.15, 0.2) ferrites have been studied as a function of frequency and applied field. The values of dielectric constant and dielectric loss have been reduced significantly due to the doping of La^{3+} ions in cobalt ferrite. The dielectric loss of the investigated ferrite is 1.9×10^{-3} at 9 MHz. The dc electrical resistivity of $CoLa_{0.1}Fe_{1.9}O_4$ ferrite was found to increase up to 30 times more as compared to pure cobalt ferrite at room temperature. Low values of dielectric constant, dielectric loss and magnetic loss can be correlated with better compositional stoichiometry and Fe ions concentration. The mechanisms responsible to these processes have been discussed.

1. Introduction

Nano-scale materials possess intriguing properties that are comparable to or superior to those of bulk. These materials are interesting due to their fascinating size dependent optical, electronic, magnetic, thermal, mechanical and chemical properties [1,2]. Cobalt ferrites have been regarded as one of the competitive candidates for high density magnetic recording media because of its moderate saturation magnetization, high coercivity, mechanical hardness and chemical stability [3]. Synthesis of nanoparticles, especially spinel ferrites, characterized by a low size distribution is important due to their remarkable electrical and magnetic properties and wide practical applications in information storage systems, ferro-fluid technology, magneto-caloric refrigeration and magnetic diagnostics [4]. Cobalt ferrites are among the most widely used magnetic materials having low cost, high performance for high frequency applications [5–8]. The properties of ferrites are very sensitive to the processing techniques. The various processing techniques, which are used for the synthesis of spinel ferrite powders, include microwave refluxing, hydrothermal, sol–gel, co-precipitation and spray pyrolysis. Cobalt ferrites prepared by different methods have different magnetic properties [9–14]. The co-precipitation method offers a synthesis route for the production of ferrite, which is uniform and non-aggregated. Though the ferrites were prepared at 100 °C, but to obtain good results, ferrite samples were sintered at 500 °C.Our interest is to make pure cobalt ferrite at nano-scale with magnetic properties similar to bulk material and then to modulate the properties by doping with La^{3+} ions. In this study we have prepared La–Co ferrites and compared the properties of $CoFe_2O_4$ and $CoLa_{0.1}Fe_{1.9}O_4$. In order to show the effect for higher concentration of La^{3+}, we have mentioned the result for $CoLa_{0.15}Fe_{1.85}O_4$ and $CoLa_{0.2}Fe_{1.8}O_4$. The room temperature saturation magnetization for pure cobalt ferrite is about 60 emu/g which is higher than achieved by sol–gel method [15]. It has been reported that [16] remanence and coercivity is not observed at 300 K for rare earth doped cobalt ferrite, however, we have been able to observe it at the temperature. In addition, we have been able to prepare La^{3+} doped samples with higher resistivity, low dielectric and magnetic losses.

2. Experimental

Lanthanum–cobalt ferrites of composition $CoLa_xFe_{2-x}O_4$ ($x = 0$, 0.1, 0.15, 0.2) were prepared by the co-precipitation method [17]. The materials used were cobalt nitrate (97% Merck, India), iron nitrate (98% Merck, India), lanthanum nitrate (Merck,

---

* Corresponding author.
E-mail address: pawankumarsolan@gmail.com (P. Kumar).

0925-8388/$ – see front matter © 2010 Elsevier B.V. All rights reserved.
doi:10.1016/j.jallcom.2010.08.007

Germany) and sodium hydroxide (96% Merck, India). These solutions were poured as quickly as possible into the boiling solution of NaOH under vigorous stirring produced by the glass mechanical stirrer (500 rpm). Mixing is very important; otherwise segregation of phases can take place. After co-precipitation, pH is set to 12.5–13. The beaker was covered to diminish the evaporation of the solution. Reaction was continued for 30–40 min at temperature 95–100 °C under vigorous stirring. The beaker was cooled to ambient temperature and particles precipitate. Precipitates were washed with distilled water and centrifuged at 7000 rpm for 10 min. The residue was dried and powdered. These samples were sintered in air at 500 °C at a heating rate of 350 °C/h for 3 h and were subsequently cooled. This powder was mixed with 2% P.V.A. binder and pressed into pellets and rings uniaxially under a pressure of 5 ton/inch^2 in a stainless steel die. These samples were then sintered in air at 500 °C for 3 h and were subsequently cooled.

The purpose of sintering is to develop the most appropriate structure for the application, complete the inter-diffusion of the component metal ions into the desired crystal lattice and to establish the appropriate valencies for the multi-valent ions by proper oxygen control [18]. Sintering is the bonding together of compacted powder particles at temperatures below the melting point. It involves the joining of particles placed in contact with each other by growth of neck at the region of contact, when the particles are heated to appropriate temperature. Sintering in practice is the control of both densification and grain growth. Densification is the act of reducing porosity in a sample thereby making it denser. Sintering is effective when the process reduces the porosity and enhances properties such as strength and thermal conductivity. The main mechanism responsible for sintering is the lattice or volume diffusion of atoms which occur through vacancy movements with grain boundaries acting as vacancy sinks. Various parameters like temperature, pressure, time and atmosphere affect the sintering process.

The rings were wound with about 42 turns of 34 SWG enameled copper wire to form the toroids. Saturation magnetization and magnetic remanence were measured by using vibrating sample magnetometer (VSM). XRD was taken with XPERT-PRO system.

Dielectric measurements and permeability studies were done with LCR meter from Agilent Technologies 4285A. The dielectric constant was determined using formula $\varepsilon' = Cd/\varepsilon_0 A$ where C is the capacitance of the pallet, d is the thickness of the pellet, A is the cross-sectional area of the flat surface of the pallet in and ε_0 is the permittivity of free space.

Initial permeability $\mu_i = L/L_0$, where L is inductance of the sample and L_0 is the inductance with air core and $L_0 = 4.6\,N^2 d \log(\mathrm{OD/ID}) \times 10^{-9}$ H, N is the number of turns, d is the thickness of toroid in metre, OD and ID are outer and inner diameters of the toroid respectively.

The tangent of dielectric loss angle can be calculated using the relation $\tan\delta = 1/2\pi f R_s C_s$ where δ is the loss angle, f is the frequency, R_s is the equivalent series resistance and C_s is the equivalent series capacitance.

The dielectric loss factor (ε'') is also measured in terms of tangent loss factor ($\tan\delta$) defined by the relation [19] $\varepsilon'' = \varepsilon' \tan\delta$, where ε' and $\tan\delta$ are defined above.

The dc resistivity of the sample was measured by using a Keithley-2611 system.

3. Result and discussion

3.1. Structural study

The X-ray diffraction patterns for the typical $\mathrm{CoLa}_x\mathrm{Fe}_{2-x}\mathrm{O}_4$ ($x = 0$, 0.1, 0.15, 0.2) ferrite powder obtained on calcination at 500 °C shows a typical single-phase inverse spinel structure and are shown in Fig. 1. The diffraction peaks are broad because of the nanometer size of the crystallite. The particle size of the samples has been estimated from the broadening of XRD peaks using the Scherrer equation [20]. The average particle size for the $\mathrm{CoFe_2O_4}$ is 49 nm and for $\mathrm{CoLa_{0.1}Fe_{1.9}O_4}$ is around 17 nm while for $x = 0.15$ and $x = 0.2$ it is 49 nm and 28 nm respectively.

3.2. Electrical resistivity

Fig. 2 shows the variation of resistivity with temperature for $\mathrm{CoFe_2O_4}$ and $\mathrm{CoLa_{0.1}Fe_{1.9}O_4}$ samples. High dc resistivity of $\sim 20.621 \times 10^6\ \Omega$ cm is obtained for $x = 0.1$ sample at room temperature and it decreases with increase in temperature. The higher value of dc resistivity is due to $\mathrm{La^{3+}}$ content in cobalt ferrite. The addition of $\mathrm{La^{3+}}$ ions in place of $\mathrm{Fe^{3+}}$ ions limits the degree of conduction by blocking Verwey's hopping mechanism, resulting in an increase of resistivity. $\mathrm{La^{3+}}$ content doping reduces the number of $\mathrm{Fe^{3+}}$ ions on the octahedral sites which play a dominant role in the mechanism of conduction [21–23]. The dc resistivity for $\mathrm{CoLa_{0.15}Fe_{1.85}O_4}$ and $\mathrm{CoLa_{0.2}Fe_{1.8}O_4}$ increases slightly [Table 1].

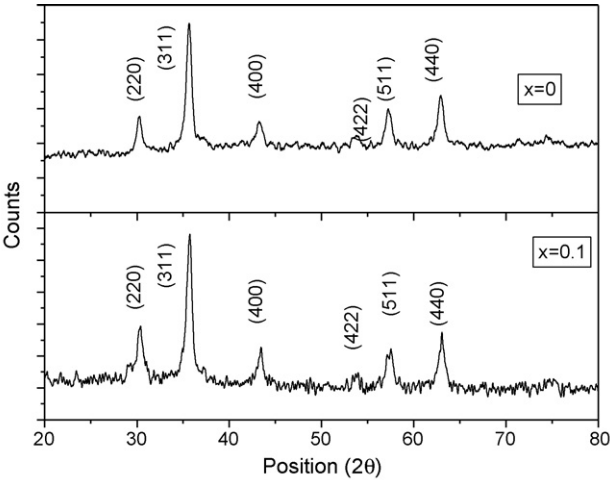

Fig. 1. XRD patterns of $\mathrm{CoFe_2O_4}$ and $\mathrm{CoLa_{0.1}Fe_{1.9}O_4}$ sintered at 500 °C.

3.3. Dielectric study

Fig. 3 shows the variation of dielectric constant as a function of frequency. The dielectric constant decreases slowly initially with frequency up to 4 MHz and remains constant up to 10 MHz. Initial decrease in dielectric constant with frequency up to 4 MHz can be explained by the phenomenon of dipole relaxation [24,25]. Dipole relaxation refers to the relaxation response of a dielectric medium to an external electric field at microwave frequencies. Relaxation, in general, is a delay or lag in the response of a system. Dielectric constant is due to the polarization of the material. The decrease of polarization of the dielectric constant with increasing frequency is due to the fact that beyond certain frequency of the electric field, the electronic exchange between $\mathrm{Fe^{2+}}$ and $\mathrm{Fe^{3+}}$ ion cannot follow the electric field. Since an assembly of space charge carriers in a dielectric requires finite time to line up their axes parallel to an alternating field. If the frequency of the alternating field increases,

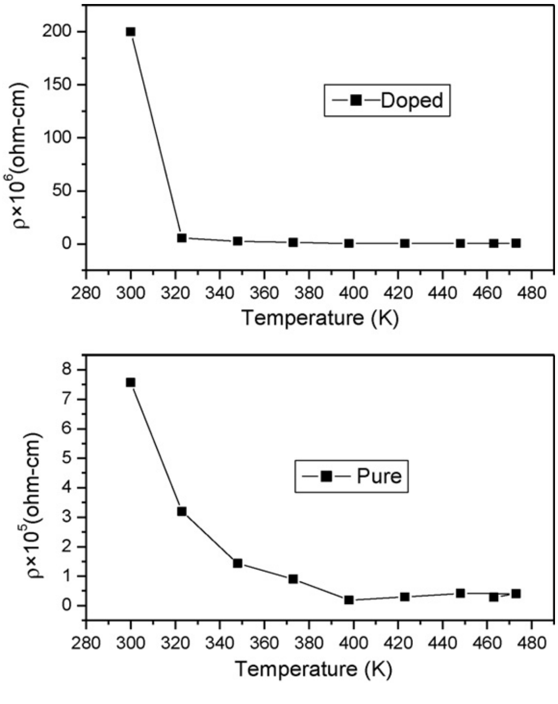

Fig. 2. Variation of resistivity of $\mathrm{CoFe_2O_4}$ and $\mathrm{CoLa_{0.1}Fe_{1.9}O_4}$ ferrites with temperature.

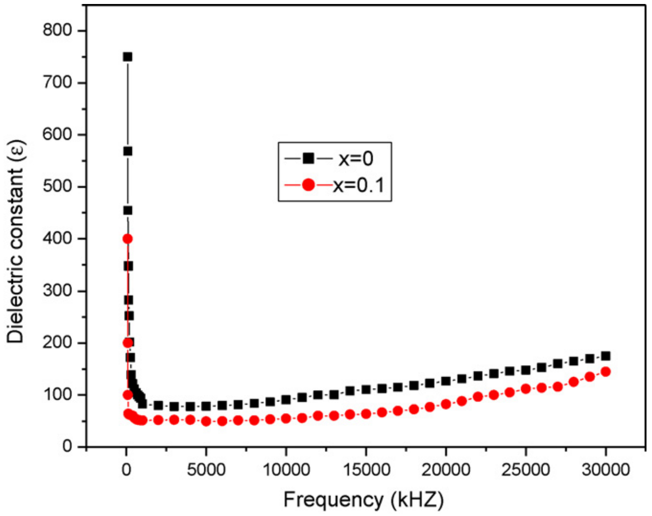

Fig. 3. Variation of dielectric constant of $CoFe_2O_4$ and $CoLa_{0.1}Fe_{1.9}O_4$ ferrites with frequency.

a point will be reached when the space change carriers cannot keep up with field and the alternation of their direction lags behind the field. As the frequency of the field continues to increase, at some stage the space charge carrier will barely have started to move before the field reverses and make almost no contribution to the polarization of the dielectric. As a result, the dielectric constant of a material may decrease substantially as the frequency is increased.

The increase in dielectric constant above 10 MHz may indicate the beginning of presence of resonance peak which occurs at higher frequency. The resonance may arise due to the matching of the frequency of charge transfer between $Fe^{2+} \leftrightarrow Fe^{3+}$ ions and that of the applied electric field.

Fig. 4 shows the variation of dielectric loss with frequency. The dielectric loss factor decreases initially with increase in frequency followed by the appearance of the resonance with peaks occurring at higher frequencies. The decrease in dielectric loss ($\tan\delta$) with increase in frequency is in accordance with the Koops phenomenological model [26]. Resonance occurs when the frequency of the applied electric field is equal to hopping frequency. Hudson [27] has shown that, the dielectric losses in ferrites is reflected in the conductivity measurements where the materials of high conductivity exhibiting higher losses and vice-versa. The value of dielectric loss observed at room temperature is only 1.9×10^{-3} at 9 MHz. The low value of dielectric constant, dielectric loss and high value of dc resistivity is due to the substitution of La^{3+} ion in cobalt ferrite as shown in Table 1. This result is explained in view of the hopping conduction mechanism between $Fe^{2+} \leftrightarrow La^{3+} + e^{-1}$. The addition of La^{3+} ions in place of Fe^{3+} ions limits the degree of conduction and polarization by blocking Verwey's hopping mechanism [28], resulting decrease in conductivity, dielectric constant and dielectric loss.

Table 1 mentions dielectric constant as well as in dielectric loss for $CoLa_{0.15}Fe_{1.85}O_4$ and $CoLa_{0.2}Fe_{1.8}O_4$.

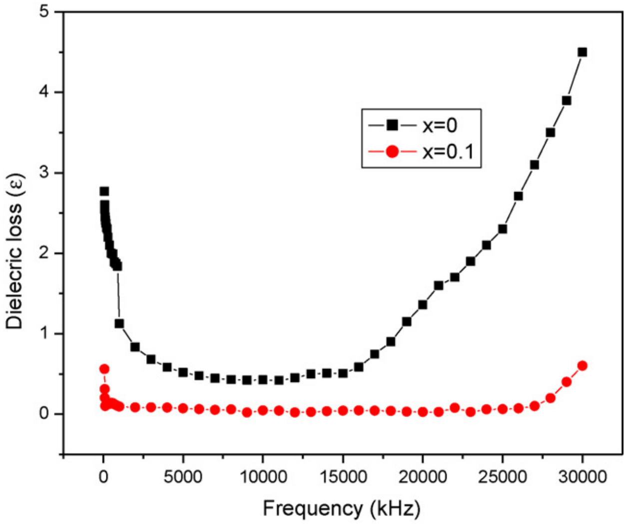

Fig. 4. Variation of dielectric loss of $CoFe_2O_4$ and $CoLa_{0.1}Fe_{1.9}O_4$ ferrites with frequency.

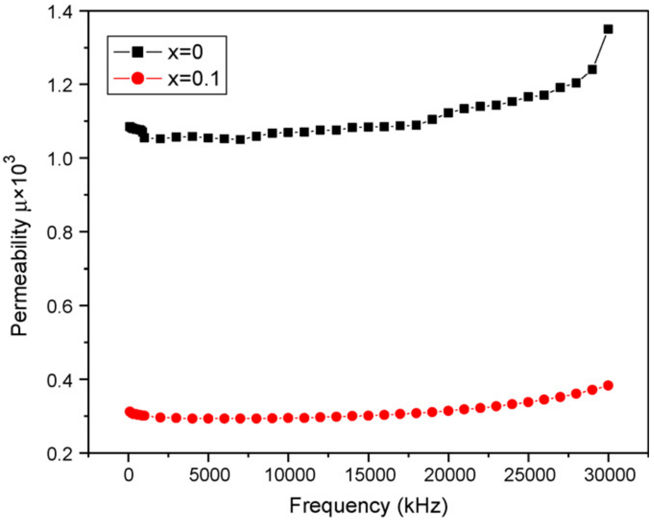

Fig. 5. Variation of permeability of $CoFe_2O_4$ and $CoLa_{0.1}Fe_{1.9}O_4$ ferrites with frequency.

3.4. Magnetic study

The typical variation of initial permeability with frequency for $x = 0$, 0.1 are shown in Fig. 5. It shows that the value of initial permeability is fairly constant over a wide range of frequency. It means the sample prepared is compositionally stable and quality-wise is also good. It makes it desirable for a variety of applications like broadband pulse transformers and wide band read write heads for video recording. However after 20 MHz permeability starts increasing and the rise indicates that at some higher frequencies the resonance will happen [29]. This happens when applied field frequency matches with precessing frequency

Table 1
Electric, dielectric and magnetic parameters of $CoLa_xFe_{2-x}O_4$ ($x = 0$, 0.1, 0.15, 0.2) sintered at 500 °C.

Composition	Resistivity ρ (Ω cm)	Dielectric loss (at 9 MHz)	Dielectric constant (9 MHz)	Magnetic loss factor (9 MHz)	Saturation magnetization (emu/g)
$x = 0$	6.465×10^5	40×10^{-3}	84.00	40×10^{-3}	60.570
$x = 0.1$	20.621×10^6	1.9×10^{-3}	67.05	25×10^{-3}	47.133
$x = 0.15$	26.990×10^6	1.5×10^{-3}	60.75	4×10^{-3}	42.104
$x = 0.2$	33.310×10^6	0.5×10^{-3}	55.61	4×10^{-3}	40.933

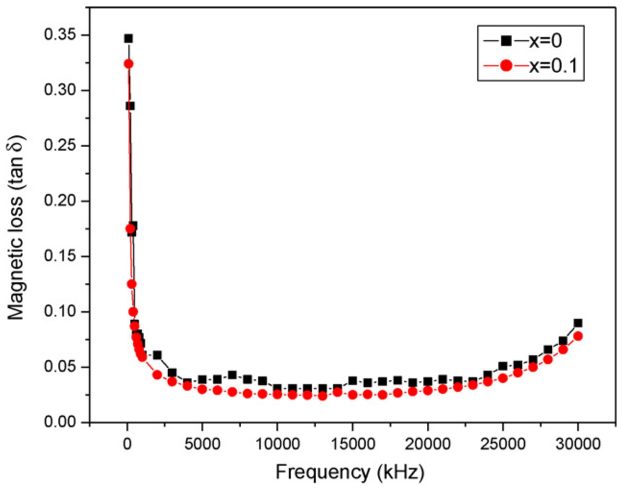

Fig. 6. Variation of magnetic loss of $CoFe_2O_4$ and $CoLa_{0.1}Fe_{1.9}O_4$ ferrites with frequency.

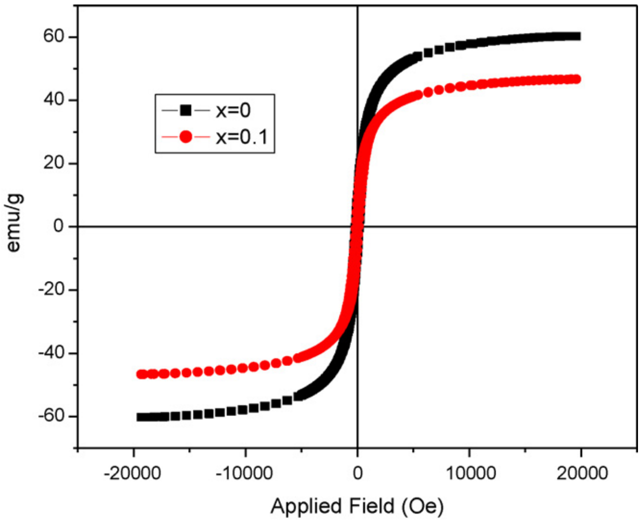

Fig. 7. *M–H* plots for $CoFe_2O_4$ and $CoLa_{0.1}Fe_{1.9}O_4$.

of magnetic spins in ferrites. This matching leads to energy transfer from the field to the ferrite system in orienting the dipoles.

Fig. 6 shows the variation of magnetic loss at different frequencies. The loss is due to the lag of domain walls with respect to the applied alternating field and is attributed to imperfections in the lattice. The magnetic loss factor ($\tan\delta$) decreases initially and it remains almost constant up to 12 MHz.The increase in $\tan\delta$ above 12 MHz may indicate the beginning of a possible presence of resonance with peaks occurring at higher frequencies.

In the ideal situation, when the sample prepared grows into a pure inverse type spinel structure with all Co^{2+} ions located in the octahedral sub-lattice, the magnetization per formula unit is represented by the net moment of that in A and B sites. A simple theoretical expression for the net moments of $CoLa_{0.1}Fe_{1.9}O_4$ can be written as (assuming La^{3+} ions assuming only the B sites for their large ion radii): $M_{La} = M_B - M_A = [5 \times 0.9 + 3.8 + 0.1 \times \mu_{La}] - 5 = 3.3 + 0.1 \times 0 = 3.3\,\mu_B$ where M_A and M_B represent the total magnetic moment of the A and B sub-lattices, respectively. The magnetic moment of Fe^{3+} cations is fixed to be 5 μ_B (spin only) and that of octahedrally coordinated Co^{2+} cations is fixed to be 3.8 μ_B which corresponds to the saturation magnetization at 0 K of bulk $CoFe_2O_4$ (95 emu/g) [16]. The net magnetic moment for La^{3+} has been taken to be zero, La^{3+} being non-magnetic. So the saturation magnetization is expected to be less than pure $CoFe_2O_4$ ($x = 0$). The measurements (Fig. 7) show that saturation magnetization decreases with the increase of La^{3+} ions. This can be related to the decrease in Fe^{3+}–Fe^{3+} (B–B) interactions resulting from doping with La^{3+} [30].

The initial permeability of spinel ferrites can be expressed as $\mu_i \alpha M_s{}^2 D_m/K_1$, where D_m is the average grain diameter, K_1 is the magneto-crystalline anisotropy constant and M_s is the saturation magnetization [31]. As μ_i is proportional to $M_s{}^2$, the variation of μ_i with x for La^{3+} should be affected in a manner similar to that of variation of $M_s{}^2$ with x. Hence the decrease of permeability and saturation magnetization with La^{3+} ions concentration can be correlated well with each other.

Saturation magnetization for $x = 0.15$, 0.2 is mentioned in Table 1.

4. Conclusions

$CoLa_xFe_{2-x}O_4$ ($x = 0, 0.1, 0.15, 0.2$) ferrites were successfully synthesized by co-precipitation method. Incorporation of La^{3+} ions results in increase in dc resistivity. High value of dc resistivity, of the order of $10^6\,\Omega$ cm, makes this ferrite suitable for the high frequency applications where eddy current losses become appreciable. The dielectric loss and magnetic loss of the prepared ferrites is quite low. Saturation magnetization decreases with concentration of La^{3+} ions concentration. The samples although in nano-range but still show appreciable hysteresis with good value of saturation magnetization and remanence at room temperature.

References

[1] J. Chand, M. Singh, J. Alloys Compd. 487 (2009) 376.
[2] S. Thakur, S.C. Katyal, M. Singh, J. Magn. Magn. Mater. 321 (2009) 1.
[3] S. Singhal, S.K. Barthwal, K. Chandra, J. Magn. Magn. Mater. 306 (2006) 233.
[4] M.J. Iqbal, M.R. Siddiquah, J. Alloys Compd. 453 (2008) 513.
[5] T.M. Whiteny, J.S. Jiang, P.C. Season, C.L. Chien, Science 261 (1993) 1316.
[6] L. Piraux, J.M. George, J.F. Despres, C. Leroy, E. Ferain, R.L. Legras, K. Ounadjela, A. Fert, Appl. Phys. Lett. 65 (1994) 2484.
[7] H.E. Zhang, B.F. Zhang, G.F. Wang, X.H. Dong, Y. Gao, J. Magn. Magn. Mater. 312 (2007) 126.
[8] J. Kulikowski, J. Magn. Magn. Mater. 41 (1974) 56.
[9] K.V.P.M. Shafi, Y. Koltypin, A. Gedanken, et al., J. Phys. Chem. B 101 (1997) 6409.
[10] S. Prasad, N.S. Gajbhiye, J. Alloys Compd. 265 (1998) 87.
[11] Y. Shi, J. Ding, X. Liu, J. Wang, J. Magn. Magn. Mater. 205 (1999) 249.
[12] A. Kale, S. Gubbala, R.D.K. Misra, J. Magn. Magn. Mater. 277 (2004) 350.
[13] J. Zhou, J. Ma, C. Sun, I. Xie, Z. Zhao, H. Tian, J. Am. Ceram. Soc. 88 (2005) 3535.
[14] M. Grigorova, H.J. Blythe, V. Blaskov, V. Rusanov, V. Petkov, V. Masheva, D. Nihtianova, L.M. Martinez, J.S. Munoz, M. Mikhov, J. Magn. Magn. Mater. 183 (1998) 163.
[15] B.G. Toksha, E. Sagar, S.M. Shirsath, K.M. Patange, Jadhav, Solid State Commun. 147 (2008) 479.
[16] L. Ben Tahar, M. Artus, S. Ammar, L.S. Smiri, F. Herbst, M.J. Vaulay, V. Richard, M. Greneche, F. Villain, F. Fievet, J. Magn. Magn. Mater. 320 (2008) 3242.
[17] P. Mathur, A. Thakur, M. Singh, Mod. Phys. Lett. B 21 (2007) 1425.
[18] Alex Goldman, Modern Ferrite Technology, 2nd ed., Springer, New York, 2006.
[19] D. Ravinder, K.V. Kumar, Bull. Mater. Sci. 24 (2001) 505.
[20] B.D. Cullity, Elements of X-Ray Diffraction, Addison-Wesley, Reading, MA, 1978.
[21] M.A. Ahmed, E. Ateia, F.M. Salem, J. Mater. Sci. 42 (2007) 3651.
[22] A.V. Ramana Reddy, G. Ranga Mohan, D. Ravinder, J. Mater. Sci. 34 (1999) 3169.
[23] M.A. Ahmed, E. Ateia, I. El-Deks, Vib. Spectrosc. 30 (2002) 69.
[24] D.H. Wang, W.C. Goh, M. Ning, C.K. Ong, Appl. Phys. Lett. 88 (2006) 212907.
[25] M. Kumar, K.L. Yadav, J. Appl. Phys. 100 (2006) 74111.
[26] C.G. Koops, Phys. Rev. 83 (1951) 121.
[27] A.S. Hudson, Marconi Rev. 37 (1978) 43.
[28] E.W. Verway, P.W. Haaijman, F.C. Romeyn, G.W. Van Oosterhont, Philips, Res. Rep. 5 (1950) 173.
[29] J.L. Snoek, Physica 14 (1948) 207.
[30] M.L. Kahn, Z.J. Zhang, Appl. Phys. Lett. 78 (2001) 3651.
[31] A. Globus, P. Duplex, M. Guyot, IEEE Trans. Magn. Magn. 7 (1991) 617.